A superspace approach to the modulated structures of $MA_xTe_2$ (M=Nb, Ta; A=Si, Ge; $^1/_3$ < or = x < or = $^1/_2$), exemplified by $NbGe_{3/7}Te_2$



1994 J. Phys.: Condens. Matter 6 933

(http://iopscience.iop.org/0953-8984/6/5/003)

J. Phys.: Condens. Matter 6 (1994) 933–944. Printed in the UK

# A superspace approach to the modulated structures of $MA_xTe_2$ (M = Nb, Ta; A = Si, Ge; $\frac{1}{3} \leqslant x \leqslant \frac{1}{2}$), exemplified by $NbGe_{3/7}Te_2$

A van der Lee†, M Evain†‡, L Monconduit†, R Brec† and S van Smaalen§

† IMN, Laboratoire de Chimie des Solides, 2 rue de la Houssinière, 44072 Nantes Cédex 03, France

§ Laboratory of Chemical Physics, Materials Science Centre, University of Groningen, Nijenborgh 4, 9747 AG Groningen, The Netherlands

Received 16 September 1993

**Abstract.** $MA_xTe_2$ (M = Ta, Nb and A = Si, Ge) compounds show a great variety of commensurately and incommensurately modulated structures depending on the value for $x$. It is shown that the theory of superspace groups can be used to standardize the structures and to predict the 3D symmetry of the commensurately modulated structures. The commensurately modulated structure of $NbGe_{3/7}Te_2$ is determined with the aid of single crystal x-ray data. A comparison with some already published structures in the series shows that all structures with $\frac{1}{3} \leqslant x \leqslant \frac{1}{2}$ can be regarded as being built from definite numbers of units of the $MA_{1/3}Te_2$ and $MA_{1/2}Te_2$ type.

## 1. Introduction

Recent studies in the M–A–Te type ternary phase system (M = Nb, Ta; A = Si, Ge) have shown that the $MA_xTe_2$ compounds are very suitable for correlated investigations of the electronic and geometric structure of transition metal tellurides [1–3]. In this case the particular point of interest is the change transfer which takes place between the transition metal element d bands and the Te p orbitals in relation to the Te–Te contact distances. The rather simple variation of $x$ in $MA_xTe_2$ and, accordingly, of the degree of the charge transfer, along with the experimental fact that nearly all structures are fairly well ordered, may lead to a better understanding of the structural variations in the M–A–Te ternary phase system and in general in the transition metal and post transition metal tellurides.

The structures to be considered range from $MA_{1/3}Te_2$ to $MA_{1/2}Te_2$, i.e. from a compound with maximal charge transfer to a compound without charge transfer. It should be noted that we use the phrase 'charge transfer' relative to the situation in which the atoms adapt their formal oxidation states, i.e. +3 for M, +2 for A, and −2 for Te. Hitherto, only structures with $\frac{1}{3} \leqslant x \leqslant \frac{1}{2}$ have been found [1, 3–7], besides the parent compounds $MTe_2$ [8], and these will be considered in this paper. It has been shown previously that the formal oxidation states of the cations remain unaltered in the modulated structures [1]. Thus, the formal oxidation state of Te becomes fractional: $-(1.5 + x)$.

Recently, it has been argued that the structures in the $MA_xTe_2$ series can be regarded as being modulated with respect to a basic unit cell common to all structures [6]. Furthermore,

‡ Author to whom correspondence should be addressed.

0953-8984/94/050933+12$07.50  

the relative magnitude of the wave vector describing the modulation has been shown to be equal to the value for $x$ in $MA_xTe_2$. This value for $x$ can be either rational ($x = n_1/n_2$, $n_1$, $n_2$ integer) or irrational, yielding a commensurate or incommensurate structure, respectively.

The superspace group approach offers a versatile and practical way to describe modulated structures [9]. It is obvious that for incommensurate structures an approach by conventional 3D space groups is not adequate, because of the absence of 3D translation symmetry. Commensurately modulated structures, however, are adequately characterized by 3D space groups by defining a new, normally larger unit cell with 3D translation symmetry. The use of superspace groups offers an alternative way of describing those commensurate structures and has several advantages compared with the conventional approach [10, 11]. Indeed, with such a description one may better compare the structures within a series with both commensurate and incommensurate modulations, such as in the $MA_xTe_2$ series. Another advantage is that in certain cases the number of independent parameters in an x-ray or neutron structure determination can be reduced as compared with the conventional approach.

In this paper we describe the use of superspace for the commensurately modulated structures of $MA_{n1/n2}Te_2$. The results can be used to standardize the structures in the series, and to foresee the symmetries of new, not yet synthesized compounds. As an example, the superspace group approach is used to determine the structure of $NbGe_{3/7}Te_2$ with the aid of single-crystal x-ray diffraction data.

## 2. Experimental procedures

$NbGe_{3/7}Te_2$ was obtained as a side product of the synthesis of $NbGe_{1/3}Te_2$ [1]. Stoichiometric amounts of the elements for the latter compound were sealed in an evacuated silica tube. The temperature of the tube was raised to 700 K and maintained for several hours, then raised to 1100 K, maintained for two days, and finally raised, step by step, to 1280 K. After ten days the tube was cooled by exposure to air. SEM analyses and Weissenberg photographs showed that not all of the thin, dark platelets found in the batch had the same composition and cell parameters. Crystals of composition $NbGe_{1/3}Te_2$, $NbGe_{2/5}Te_2$, and $NbGe_{3/7}Te_2$ were most frequently found, with the $c$ axes of the orthorhombic unit cell very close to the ratio 3:5:7, respectively. The diffraction patterns of all three compounds showed strong main spots defining an identical basic lattice with almost equal cell parameters. In between the main spots much weaker superstructure reflections were found.

For the study of $NbGe_{3/7}Te_2$, five crystals were selected and analysed by SEM, yielding an average composition of $Nb_{2.95(5)}Si_{0.40(5)}Ge_{0.62(2)}Te_{6.0(2)}$. It is quite possible that the compound is contaminated with Si from the inner walls of the silica tube. Therefore, syntheses were also performed in Si-free environments. SEM analyses of crystals resulting from these syntheses still yielded small amounts of Si. This shows that the detector of the SEM apparatus is probably contaminated with tiny amounts of Si. In any case, the results of this study will hardly be influenced by the eventual presence of Si, since Ge can easily be substituted by Si on the same crystallographic sites.

Data collection was performed on a SIEMENS-P4 diffractometer (see table 1 for the recording conditions). The measured intensities were corrected for the scale variation, Lorentz and polarization effects. A Gaussian absorption correction was applied using the program SHELXTL, distributed along with the SIEMENS-P4 diffractometer software. The intensities showed *mmm* Laue symmetry and were averaged accordingly. All

**Table 1.** Crystal data for $NbGe_{3/7}Te_2$ and conditions of measurement.

| | |
|---|---|
| Formula | $NbGe_{0.4286}Te_2$ |
| Formula weight | 379.2 g $mol^{-1}$ |
| Density (calc.) | 7.152 |
| Linear absorption coefficient | 236.6 $cm^{-1}$ |
| Maximum transmission | 0.963 |
| *Minimum transmission* | 0.306 |
| Crystal size | $< 0.24 \times 0.0016 \times 0.24$ $mm^3$ |
| Superspace group | $Pnma(00\gamma)s00$ |
| Basic unit cell | $a = 6.435(1)$ Å |
| | $b = 14.006(2)$ Å |
| | $c = 3.9072(4)$ Å |
| Modulation vector | $q = \frac{3}{7}c^*$ |
| Diffractometer | SIEMENS-P4 |
| Temperature | 295 K |
| Radiation | Mo K$\alpha$ |
| Scan mode | $\omega$ |
| Recording range | 1.50–37.50° |
| *hklm* range | $-1 < h < 12$ |
| | $-1 < k < 24$ |
| | $-1 < l < 7$ |
| | $-3 < m < 3$ |
| Standard reflections | 002, 060, 301 every 100 reflections |

refinements were performed with the computing system JANA93 [12]. The scattering factors for neutral atoms and the anomalous dispersion correction were taken from [13]. All refinements were based on $|F_{obs}|$ and performed in the full-matrix mode, using $w = 1/(\sigma^2(|F_{obs}|) + 0.02|F_{obs}|^2)$ as weights. The definitions of the $R$-factors are $R = \sum ||F_{obs}| - |F_{cal}|| / \sum |F_{obs}|$; $wR = \left[\sum w(|F_{obs}| - |F_{cal}|)^2 / \sum w|F_{obs}|^2\right]^{1/2}$.

## 3. Symmetry and superspace

All the spots from the diffraction pattern of the structure of $NbGe_{3/7}Te_2$ can be indexed with just three integers ($hkl$) by using the smallest possible reciprocal unit cell (figure 1) with reciprocal axis $c_s^*$. The extinctions in the pattern point to the space group $Pnma$, the same as was reported for the structures of $MA_{1/3}Te_2$ [1,3–5]. The latter structures have been determined without making use of the superspace group approach.

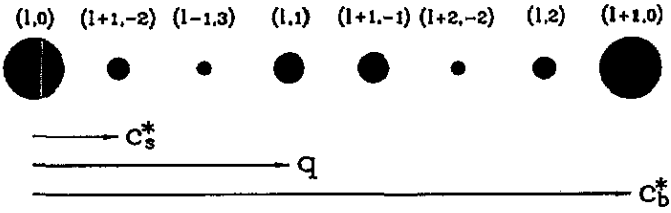


**Figure 1.** A diffraction pattern for the structure of $NbGe_{3/7}Te_2$ in between two main spots along the reciprocal $c^*$ axis. The relative size of the spots corresponds roughly to the relative intensities for each class of spots. Indexing is according to the indicated $q$-vector; for clarity $hk$ sets are omitted in each quartet of indices.

Since every seventh spot along $c_s^*$ is strong compared with the spots in between, one can alternatively assign four integers $(hklm)$ to every spot, regarding the fourth index $m$ as the order of the satellite with respect to the strong or main spots. The diffraction pattern is then indexed by

$$H = ha^* + kb^* + lc_b^* + mq \qquad q = (n_1/7)c_b^*. \tag{1}$$

*A priori*, the choice of $n_1$ is ambiguous, since the diffraction pattern is completely indexed with integer indices $(hklm)$ for any value $n_1$, $n_1 \in (1 \ldots 6)$. The natural choice seems to be the one which assigns the strongest satellites to the first order $m = 1$; this corresponds in our case to $q = (3/7)c_b^*$. When indexed according to this choice, the (3+1)D superspace group matching the set of extinction rules is $Pnma(00\gamma)s00$. (Equivalent to No 62.1 in table 9.8.3.5 of [14].) Other choices for $q$ may lead to other settings of the superspace group, and always give the same structure. $Pnma(00\gamma)s00$ was also reported for the incommensurate structure of $TaSi_{0.360}Te_2$ with wave vector $q = 0.360c^*$ [6]. Table 2 gives the (3+1)D symmetry operations for this superspace group.

**Table 2.** Symmetry operations of the superspace group $Pnma(00\gamma)s00$. The superspace group operators are written as $(R\epsilon \mid \nu_1\nu_2\nu_3\nu_4)$ where $R$ is the 3D rotational part, $\epsilon$ the (1D) rotational part acting on the fourth coordinate, $(\nu_1\nu_2\nu_3\nu_4)$ the (3+1)D translational part, and $\nu_4 = \delta - \nu_4'$. $n_i$, $i = 1 \ldots 4$, are integers.

| | |
|---|---|
| $(E\mathbf{1} \mid n_1, n_2, n_3, n_4)$ | $(i\bar{\mathbf{1}} \mid \nu_1, \nu_2, \nu_3, \nu_4')$ |
| $(m_x\mathbf{1} \mid \frac{1}{2} + \nu_1, \frac{1}{2}, \frac{1}{2}, \frac{1}{2})$ | $(2_x\bar{\mathbf{1}} \mid \frac{1}{2}, \frac{1}{2} + \nu_2, \frac{1}{2} + \nu_3, \frac{1}{2} + \nu_4')$ |
| $(m_y\mathbf{1} \mid 0, \frac{1}{2} + \nu_2, 0, 0)$ | $(2_y\bar{\mathbf{1}} \mid \nu_1, \frac{1}{2}, \nu_3, \nu_4')$ |
| $(2_z\mathbf{1} \mid \frac{1}{2} + \nu_1, \nu_2, \frac{1}{2}, \frac{1}{2})$ | $(m_z\bar{\mathbf{1}} \mid \frac{1}{2}, 0, \frac{1}{2} + \nu_3, \frac{1}{2} + \nu_4')$ |

Employing the superspace group approach, one has to use periodic functions to describe the displacive and/or occupational probability modulations that are present in the structure:

$$r^\nu(\bar{x}_4) = r_0^\nu + \sum_{n=1}^{ntot}[u_{s,n}^\nu \sin(2\pi n\bar{x}_4) + u_{c,n}^\nu \cos(2\pi n\bar{x}_4)] \tag{2}$$

$$P^\nu(\bar{x}_4) = P_0^\nu + \sum_{n=1}^{ntot}[P_{s,n}^\nu \sin(2\pi n\bar{x}_4) + P_{c,n}^\nu \cos(2\pi n\bar{x}_4)] \tag{3}$$

where $\nu$ counts the independent atoms in the basic unit cell, $n$ is the order of the harmonic ($\leqslant ntot$), $\bar{x}_4$ is the argument of the modulation function: $\bar{x}_4 = t + q \cdot r_{0,L}^\nu = t + q \cdot (r_0^\nu + L)$, with $t$ the global phase of the modulation wave, $r_0^\nu$ the average position within the basic unit cell, $L$ a basic structure lattice translation, and $u_{s,n}^\nu = (A_{x,s,n}^\nu, A_{y,s,n}^\nu, A_{z,s,n}^\nu)$, $u_{c,n}^\nu = (A_{x,c,n}^\nu, A_{y,c,n}^\nu, A_{z,c,n}^\nu)$.

For incommensurately modulated structures $\bar{x}_4$ takes all possible values between 0.0 and 1.0 (mod 1). Thus, the variation of $t$ yields an infinite number of identical structures, differently localized in space. For commensurately modulated structures, however, $\bar{x}_4$ is restricted to a finite number of, say $N$, values. Only a shift of the global phase $t$ of $1/N$ produces the same 3D structure. Let $(R\epsilon \mid \nu_1\nu_2\nu_3\nu_4)_i$ be a (3+1)D symmetry operation, with $\nu_4 = \delta - \nu_4'$ where $\delta$ is an intrinsic phase-independent shift and $\nu_4'$ is a phase-dependent shift. A condition can be derived for the (3+1)D symmetry operation to be a 3D symmetry

operation by requiring that the same relation must exist between symmetry related atoms in the (3+1)D description and those in the 3D description:

$$t(\epsilon_i - 1) = \boldsymbol{q} \cdot (\boldsymbol{\nu}_i + \boldsymbol{L}) - \nu_{4,i} \qquad (\text{mod } 1) \qquad \boldsymbol{\nu}_i = (\nu_1, \nu_2, \nu_3)_i. \tag{4}$$

Alternatively, one can use equation (4) to find the 3D space group if the superspace group is known. For operations with $\epsilon = 1$, $\nu_4$ is fixed and independent of $t$. For operations with $\epsilon = -1$, $\nu_4$, or more precisely $\nu_4'$, is related to $t$, through

$$t = \tfrac{1}{2}[\delta_i - \nu_{4,i}' - \boldsymbol{q} \cdot (\boldsymbol{\nu}_i + \boldsymbol{L})] \qquad (\text{mod } \tfrac{1}{2}). \tag{5}$$

Different 3D structures are obtained by either varying $t$ and setting $\nu_4' = 0$ or by varying $\nu_4'$ and setting $t = 0$. The relation between the two approaches is given by the relation between $t$ and $\nu_4'$ : $t = \frac{1}{2}\nu_4'$. With the choice $t = 0$ and $\nu_4'$ variable, the condition limiting the possible 3D symmetry elements is the same for operations with $\epsilon = 1$ and $\epsilon = -1$, namely

$$\nu_{4,i} = \boldsymbol{q} \cdot (\boldsymbol{\nu}_i + \boldsymbol{L}) \qquad (\text{mod } 1). \tag{6}$$

This last expression is the same as was previously reported by Yamamoto and Nakazawa [15] in a slightly different notation. With the operations given in table 2 and equation (6) all possible 3D space groups have been calculated assuming a general commensurate wave vector $\boldsymbol{q} = (n_1/n_2)\boldsymbol{c}^*$. These space groups have been compiled in table 3. The results show that the 3D space group symmetry is lower than *Pnma* if one of the components $n_1$, $n_2$ of the modulation vector is even and the other odd.

**Table 3.** 3D space groups derived from the (3+1)D superspace group $Pnma(00\gamma)s00$ by virtue of the condition $\nu_4 = \boldsymbol{q} \cdot (\boldsymbol{\nu}_i + \boldsymbol{L})$ (mod 1), with $\boldsymbol{q} = (n_1/n_2)\boldsymbol{c}^*$.

| | $\nu_4' = 0$ (mod $\frac{1}{n_2}$) | Otherwise |
|---|---|---|
| $n_1 + n_2 =$ even | *Pnma* | $Pnm2_1$ |

| | $\nu_4' = 0$ (mod $\frac{1}{n_2}$) | $\nu_4' = \frac{1}{2n_2}$ (mod $\frac{1}{n_2}$) | Otherwise |
|---|---|---|---|
| $n_1 + n_2 =$ odd[a] | $P2_1/m$ | $P2_1ma$ | *Pm* |

[a] $n_1$ = odd, $n_2$ = even gives the same 3D space groups as $n_1$ = even, $n_2$ = odd.

## 4. Refinement of the structure of $NbGe_{3/7}Te_2$

The determination of the structure of $NbGe_{3/7}Te_2$ began with a refinement of the basic structure with main reflections only. The final agreement factors are $R = 0.207$ and $wR = 0.252$. These rather high values indicate large modulations. This is also reflected in the high isotropic Debye–Waller parameters (> 1.0) for all atoms. Indeed, on refining anisotropic Debye–Waller parameters, a great improvement in the $R$-factors was obtained ($R = 0.083$, $wR = 0.104$). This shows that the Debye–Waller parameters are able to cover much of the displacive modulation in the structure. Isotropic Debye–Waller parameters were therefore used in the beginning of the refinement of the modulated structure so as not to bias the parameters of the displacive modulation.

The determination of the modulated structure began with the refinement of the first-order Fourier components of the displacive modulation of Te and of the occupation probability modulation of Nb(1) and Nb(2). The latter were restricted to each other so as to result in an occupation probability sum $P(\mathrm{Nb}(1)) + P(\mathrm{Nb}(2)) = 1.00$ for each value for $\bar{x}_4$ [6]. The refinement of these parameters resulted in a decrease of the $R$-factors comparable to the decrease obtained by refining the anisotropic Debye–Waller parameters in the average structure. The introduction of the second- and third-order harmonics of the modulation waves showed, however, that it was necessary to reverse the signs of all Fourier amplitudes to obtain a proper occupation probability distribution, i.e. values close to 1.00 and 0.00. Finally, the parameters of the displacive waves of Nb(1) and Nb(2) and all modulation parameters of Ge were refined. It is noted that the number of independent parameters for the displacive waves of the cations is lower than the seven allowed by symmetry, because the number of independent cation sites in the superstructure is lower than seven, i.e. four, three, and three for Nb(1), Nb(2) and Ge, respectively. The choice of this limited number of harmonics is to some extent arbitrary, but one should avoid taking functions that are linearly dependent on each other. The omission of second-order harmonics in the refinement is proven to work rather well, but the simultaneous refinement of the mean (i.e. the zeroth-order harmonic) and the first- and third-order harmonics easily leads to a close to singular matrix and false minima. This is certainly not advisable in the early stages of the refinement.

Although the trend of the cationic occupational probabilities in the superstructure approached a fully ordered model, the deviations from the ideal values 1.00 and 0.00 were too important to be ignored. These deviations amounted to 0.20 for certain sites, but for no site were negative densities found. The origin of this apparent disorder was sought in the existence of two domains with an equivalent, fully ordered distribution of cations. Such domains are energetically equally favourable, but apparently they do not occur in equal proportions [3]. The domains are related to each other by a mirror plane at $x \simeq \frac{1}{6}$. A similar phenomenon was found and successfully modelled in the structure of $TaSi_{1/3}Te_2$ [3]. The values for the Fourier amplitudes of the occupation probability waves were recalculated to yield a fully ordered cationic distribution in a single domain and proper constraints were set between all equal parameters of the two mirror-related domains. The $x$-parameter of the mirror was refined by means of a dummy atom. The refined domain volume fractions were 0.943(3) and 0.057(3). It is quite possible that there are other domains that take part in the structural disorder, but the volume fractions are too small to be modelled. The final agreement factors for this model are $R = 0.047$, 0.075, 0.113, 0.122 and 0.065 ($wR = 0.053$, 0.088, 0.148, 0.159, 0.074) for 463 main reflections, 587 first-order, 115 second-order, and 91 third-order satellites, in total 1256 reflections (only reflections with $I > 2.5\sigma(I)$ were used in the refinements). These $R$-factors are comparable to those resulting from the single-domain structure and 'relaxed' Fourier amplitudes for the occupation probability waves. The results for the refinements have been compiled in tables 4–6.

## 5. Discussion

From the parameters in tables 4 and 5, and equations (2) and (3), the coordinates of all atoms in the modulated structure can be generated. Since the structure is commensurate with $q = \frac{3}{7}c_b^*$, only seven basic translations along the $c$ axis are considered. The structure of $NbGe_{3/7}Te_2$ is based upon an AA/BB stacking of Te sheets perpendicular to the $b$ axis. Nb and Ge occupy sites within every other Te–Te double layer; therefore the structure is better described as an A$\alpha$A/B$\beta$B stacking of Te–cation–Te sandwiches.

**Table 4.** Final values for the amplitudes of the displacive modulation functions. The table also contains basic structure parameters ($n = 0$). Experimental standard deviations are shown in parentheses. The position of the mirror relating the two domains was determined to be $x = 0.168(1)$. The volume fraction of the main domain is 0.943(3). The z coordinates of Nb(1) and Nb(2) were restricted to each other.

| $\nu$ | $n$ | $A^{\nu}_{x,s,n}$ | $A^{\nu}_{y,s,n}$ | $A^{\nu}_{z,s,n}$ | $A^{\nu}_{x,c,n}$ | $A^{\nu}_{y,c,n}$ | $A^{\nu}_{z,c,n}$ |
|---|---|---|---|---|---|---|---|
| Nb(1) | | | | | | | |
| | 0 | | | | 0.3186(3) | 0.25 | −0.0419(3) |
| | 1 | 0.008(6) | 0.0 | −0.004(1) | 0.0110(6) | 0.0 | 0.054(1) |
| | 2 | 0.0 | 0.0 | 0.0 | 0.0 | 0.0 | 0.0 |
| | 3 | 0.0 | 0.0 | 0.0 | 0.0063(6) | 0.0 | 0.020(3) |
| Nb(2) | | | | | | | |
| | 0 | | | | 0.0324(3) | 0.25 | −0.0419 |
| | 1 | 0.0028(8) | 0.0 | 0.012(1) | −0.0013(6) | 0.0 | −0.044(1) |
| | 2 | 0.0 | 0.0 | 0.0 | 0.0 | 0.0 | 0.0 |
| | 3 | 0.0 | 0.0 | 0.0 | 0.0 | 0.0 | 0.0 |
| Ge | | | | | | | |
| | 0 | | | | 0.427(1) | 0.25 | 0.258(3) |
| | 1 | 0.0029(8) | 0.0 | −0.035(2) | −0.005(1) | 0.0 | −0.004(2) |
| Te | | | | | | | |
| | 0 | | | | 0.1681(2) | 0.11604(6) | 0.4775(2) |
| | 1 | −0.0317(2) | −0.0006(2) | −0.0063(5) | −0.0298(3) | 0.0009(2) | 0.0106(5) |
| | 2 | 0.0095(4) | −0.0012(3) | −0.0020(7) | −0.0015(4) | 0.0003(3) | 0.0197(4) |
| | 3 | 0.0108(6) | −0.0024(6) | −0.0144(6) | −0.0081(5) | −0.0003(5) | −0.0054(9) |

**Table 5.** Values for the amplitudes of the occupation probability modulation waves. The values have been calculated so as to give a fully ordered distribution of cations, i.e. a site is empty ($P = 0.00$) or occupied ($P = 1.00$). The values for Nb(2) follow from those of Nb(1) (see text).

| | $n$ | $P^{\nu}_{s,n}$ | $P^{\nu}_{c,n}$ |
|---|---|---|---|
| Nb(1) | | | |
| | 0 | | 0.571 429 |
| | 1 | 0.5437 | −0.3414 |
| | 2 | 0.1428 | 0.0689 |
| | 3 | −0.0255 | 0.2279 |
| Ge | | | |
| | 0 | | 0.428 571 |
| | 1 | −0.1278 | 0.6291 |
| | 2 | −0.0619 | 0.1460 |
| | 3 | 0.1296 | −0.1889 |

Figure 2 shows a projection of one AαA sandwich along the perpendicular direction. The BβB sandwich is related by symmetry and need not be considered separately. Nb is situated in trigonal prismatic holes, whereas Ge is found in the middle of faces joining two trigonal prisms. The trigonal prismatic coordination of Nb is very common in chalcogenides; the square coordination of Ge, perpendicular to the sandwich, is unknown except in this $MA_xTe_2$ series. All Nb atoms, except two (per sandwich), are bonded to one other (distances in the range 2.818–2.949 Å); there are thus six Nb–Nb pairs and two lone Nb atoms per sandwich. Besides the square coordination by Te (square perpendicular to the sheets), Ge is also approximately square coordinated by Nb, in this case with the coordination plane parallel to the sandwich (range: 2.756–2.847 Å). Note that the 'lone' Nb atoms form in-plane zigzag strips perpendicular to the $c$ axis, and accordingly to the running direction of

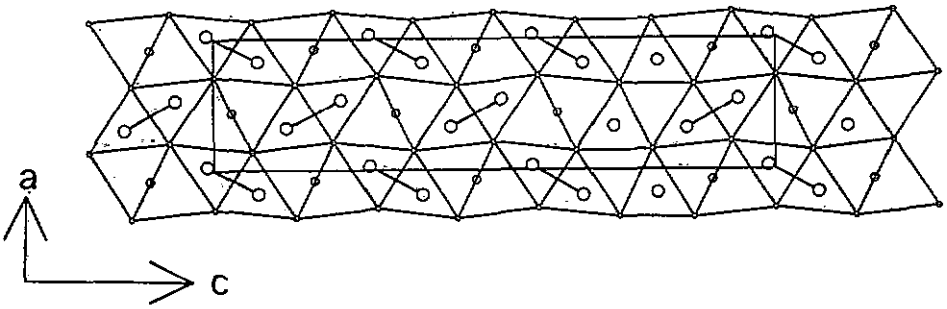


**Figure 2.** A projection of one sandwich of the structure $NbGe_{3/7}Te_2$ onto the plane $y = \frac{1}{4}$. Large open circles represent Nb, middle-sized circles Ge, and the small circles Te.

the modulation wave. The important interatomic distances in the structure of $NbGe_{3/7}Te_2$ are compiled in table 7. What is interesting is the large spread in, especially, the Te–Te contacts parallel to the layer. This is attributed to the rather diffuse character of the p orbitals of Te compared with, for instance, the other chalcogens S and Se [16].

**Table 6.** Final values for the thermal parameters. The form of the temperature factor is $\exp[-(\beta_{11}h^2 + \beta_{22}k^2 + \beta_{33}l^2 + \beta_{12}hk + \beta_{13}hl + \beta_{23}kl)]$. The standard deviation is given in parentheses.

| | $\beta_{11}$ | $\beta_{22}$ | $\beta_{33}$ | $\beta_{12}$ | $\beta_{13}$ | $\beta_{23}$ |
|---|---|---|---|---|---|---|
| Nb(1) | 0.0007(3) | 0.000 61(6) | 0.0090(8) | 0.0 | 0.0008(6) | 0.0 |
| Ge | 0.0040(6) | 0.0016(2) | 0.019(2) | 0.0 | 0.000(1) | 0.0 |
| Te | 0.0017(2) | 0.000 62(4) | 0.0101(4) | 0.000 06(9) | −0.0000(3) | −0.0000(1) |

**Table 7.** Main interatomic distances in the structure of $NbGe_{3/7}Te_2$. $\langle d \rangle$ is the mean of all closest contacts found in the structure; $\sigma_{\langle d \rangle}$ refers to the standard deviation of the mean, thus not to the usual crystallographic experimental standard deviation; $d_{min}$ and $d_{max}$ are the minimal and maximal distance, respectively, found in each set. All distances are in Å.

| | Nb–Nb | Nb–Ge | Nb–Te | Ge–Te | Te–Te (1)[a] | Te–Te (2)[b] | Te–Te (3)[c] |
|---|---|---|---|---|---|---|---|
| $\langle d \rangle$ | 2.887 | 2.801 | 2.864 | 2.770 | 3.949 | 3.823 | 3.753 |
| $\sigma_{\langle d \rangle}$ | 0.066 | 0.032 | 0.064 | 0.032 | 0.150 | 0.246 | 0.061 |
| $d_{min}$ | 2.818 | 2.756 | 2.763 | 2.728 | 3.739 | 3.306 | 3.625 |
| $d_{max}$ | 2.945 | 2.847 | 2.964 | 2.800 | 4.211 | 4.102 | 3.817 |

[a] Te–Te contacts through the van der Waals' gap, i.e. joining two different sandwiches.
[b] Te–Te contacts parallel to the layers, i.e. within one Te sheet.
[c] Te–Te contacts through a sandwich, i.e. joining the two Te sheets constituting one sandwich.

The coordination of the atoms in $NbGe_{3/7}Te_2$, i.e. bond distances and bond angles, is very near to that in $NbGe_{1/3}Te_2$ ($q = \frac{1}{3}c^*$) [1]. Thus, the two structures are very similar with regard to their stereochemistry, despite the large difference between their unit cells. It is recalled that the incommensurate structure of $TaSi_{0.360}Te_2$ ($q = 0.360c^*$) [6] was shown to consist of two building blocks, the $TaSi_{1/2}Te_2$ unit and the $TaSi_{1/3}Te_2$ unit. These two blocks consist of two and three subunits, respectively. The $TaSi_{1/3}Te_2$ unit is equal to the $TaSi_{1/2}Te_2$ unit except for an extra subunit with the lone Ta atoms (the 'zigzag' strip). The

geometric parameters of the separate building blocks, i.e. bond distances and angles, hardly change upon joining them together to create a new (in)commensurately modulated structure. Because of these observations it seems worthwhile to use similar building blocks also for the structure of $NbGe_{3/7}Te_2$, and more generally, for the whole series $MA_xTe_2$.

Considering only one sandwich, for instance $A\alpha A$, the following picture emerges (figure 3). Structures with $\frac{1}{3} \leqslant x \leqslant \frac{1}{2}$ can be considered as ordered mixtures of the two structures at the extremities of the interval, i.e. $MA_{1/3}Te_2$ and $MA_{1/2}Te_2$. The most simple commensurate structure after $MA_{1/3}Te_2$, $MA_{2/5}Te_2$, is just the combination of the two building blocks, whereas the structure determination of this paper shows that $MA_{3/7}Te_2$ is to be considered as one $MA_{1/3}Te_2$ unit plus two $MA_{1/2}Te_2$ units. In this way, a whole cascade of commensurate structures can be formed, corresponding to the general formula $MA_{(1+n)/(3+2n)}Te_2$, where $n$ is equal to the number of $MA_{1/2}Te_2$ units. The value for $(1+n)/(3+2n)$ can be shown to be exactly equal to the relative magnitude $\gamma$ of the modulation wave vector $q = \gamma c^*$ [6]. The denominator $(3+2n)$, is just the multiplification factor of the supercell with respect to the basic unit cell in the $c$ direction. This number is always odd, since it represents the combination of one $MA_{1/3}Te_2$ block consisting of three subunits and $n$ $MA_{1/2}Te_2$ blocks consisting of two subunits. The nominator, $(1+n)$, takes any integer value and defines the position of the strongest satellites in between the main reflections of the average structure, in other words, the $(1+n)$th satellite with respect to a main reflection is strong.

In between these commensurate structures, incommensurate structures are found for which the insertion of $MA_{1/2}Te_2$ units is more variable, but always 'quasi-periodic', since the diffraction pattern shows well defined spots. Alternatively, one can consider the incommensurate structures in between two successive commensurate structures $MA_{(1+n)/(3+2n)}Te_2$, say $n$ and $n+1$, as being built from the complete blocks $n$ and $n+1$. Every 'incommensurate' value $\gamma$ can be approximated by a rational value $n_1/n_2$, e.g. the structure of $TaSi_{0.360}Te_2$ has $\gamma = 0.360$ [6], which is equal to $\frac{9}{25}$. There is, however, no integer value $n$ for which $(1+n)/(3+2n)$ equals $\frac{9}{25}$. Therefore, the description of the structure of $TaSi_{0.360}Te_2$ as incommensurate is preferred as compared with a commensurate description within a 25-fold supercell.

Since the building blocks are commensurate superstructures themselves, of the same basic unit cell, in principle only one superspace group, namely $Pnma(00\gamma)s00$, is needed to describe the symmetry of the whole $MA_xTe_2$ series. Individual members of the series are completely characterized by the value for $x$, or equivalently, by the value for the wave vector $q = \gamma c^* = xc^*$.

As was shown before (table 3), the 3D space group of commensurate structures with either $n_1$ or $n_2$ even in $q = (n_1/n_2)c^*$ and superspace group symmetry $Pnma(00\gamma)s00$ is expected to have lower symmetry than the highest symmetry possible, namely $Pnma$. Although it is possible to have orthorhombic structures with either $n_1$ or $n_2$ even, via another setting of this superspace group, these structures have not been found up to now. The structures of $NbSi_{1/2}Te_2$ ($q = \frac{1}{2}c^*$) [7] and of $NbGe_{2/5}Te_2$ ($q = \frac{2}{5}c^*$) [17] consist of a number of domains of monoclinic symmetry, $P2_1/c$ for $NbSi_{1/2}Te_2$ and $P2_1/n$ for $NbGe_{2/5}Te_2$. These space groups are not found in table 3, and accordingly the superspace group symmetry cannot be $Pnma(00\gamma)s00$. On the other hand, all known phases with $q = (n_1/n_2)c^*$, $n_1$ and $n_2$ odd, have the 3D space group $Pnma$, corresponding to a value $v_4' = 0 \pmod{\frac{1}{n_2}}$.

It is insufficient to consider only one sandwich to understand the structural origin of this symmetry lowering (compared with the highest symmetry possible $Pnma$). Since the structures are thought to consist of two rigid units in which the geometric parameters

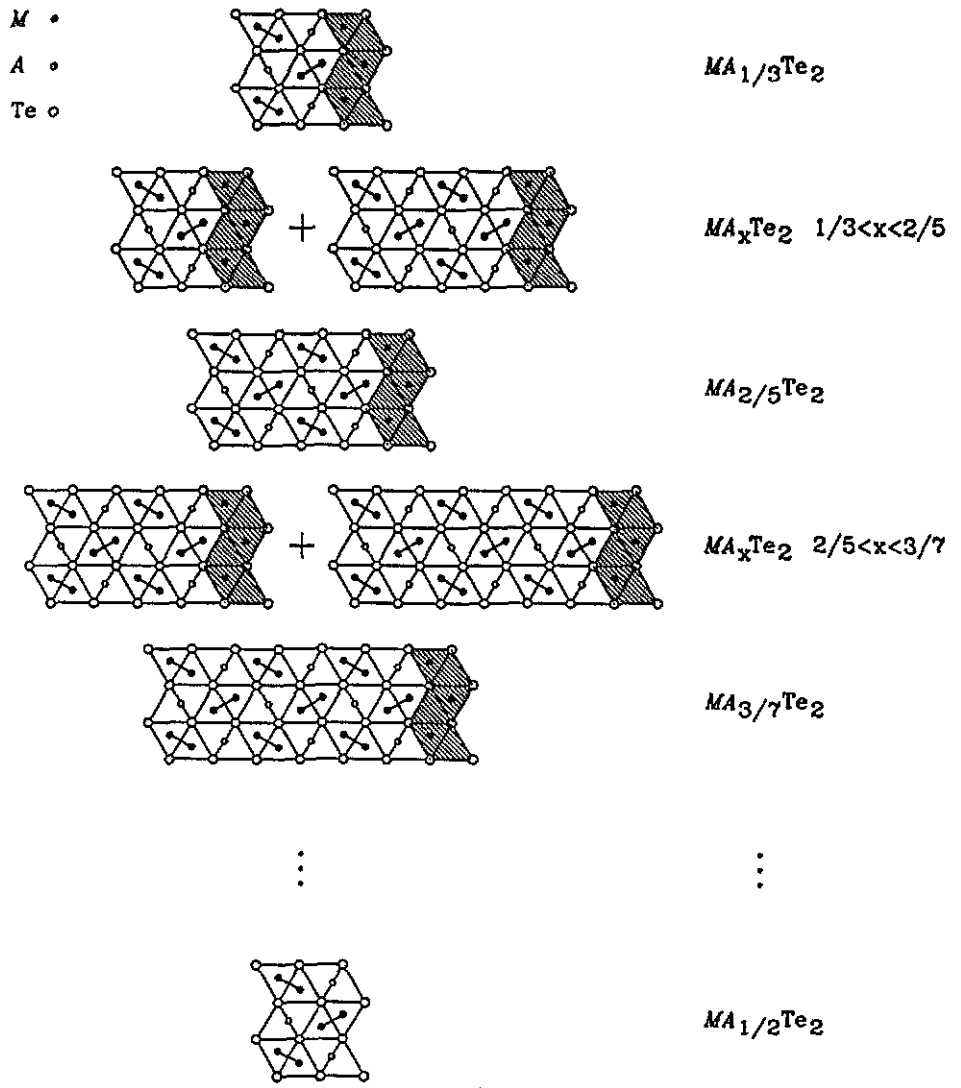


**Figure 3.** A schematic pattern of $MA_xTe_2$ ($\frac{1}{3} \leqslant x \leqslant \frac{1}{2}$) structures. The + sign for the incommensurate structures means that the structure consists of an ordered arrangement of the two units shown. The distortion of the Te network has not been taken into account for sake of clarity.

remain approximately the same after combination into a certain structure, a hypothetical orthorhombic structure for $MA_{2/5}Te_2$ can be easily constructed. In figure 4 the projection of two Te sheets of two adjacent sandwiches, i.e. those that span the empty van der Waals' gap, are shown. For comparison, the same is done for the real orthorhombic structure of $NbGe_{3/7}Te_2$. It is seen that the wavy patterns of the Te–Te vectors are more in phase for $NbGe_{3/7}Te_2$ than they are for $NbGe_{2/5}Te_2$. The structural origin of the symmetry lowering is thus a mismatching of the rigid prototype units along the stacking direction of the sandwiches. An alignment of the two Te sheets can be regained upon shifting the second sandwich in the running direction of the modulation wave, for $NbGe_{2/5}Te_2$,

over a distance of exactly two basic unit cells. This, of course, lowers the symmetry to monoclinic. Although this is not a real explanation for the symmetry lowering of the structure of $NbGe_{2/5}Te_2$, it clearly demonstrates that the structure is likely to change for either $n_1$ or $n_2$ even. A full account of the structure determination of $NbGe_{2/5}Te_2$ will be presented elsewhere [17].

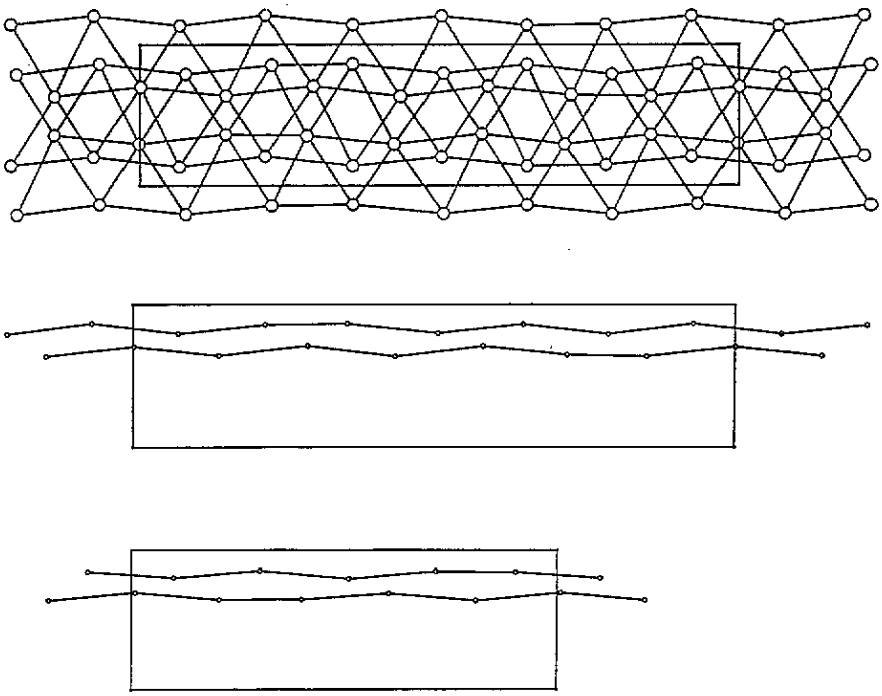

**Figure 4.** The wavy pattern of the two Te sheets that span the van der Waals' gap. The upper drawing shows the projection of the two sheets of $NbGe_{3/7}Te_2$ onto $y = \frac{1}{2}$ with all Te atoms indicated. The second drawing is the same as the first one, but for the omission of a number of atoms, to demonstrate the matching pattern more clearly. The third drawing is similar to the second, but now for hypothetical orthorhombic $NbGe_{2/5}Te_2$.

## 6. Concluding remarks

In this paper we have shown that the theory of superspace groups offers a convenient way to standardize the (in)commensurately modulated structures within the $MA_xTe_2$ phase system. Commensurately modulated structures in the series might have different 3D space groups, but the same (3+1)D superspace group which is common to that of the incommensurate structures. The structure determination of $NbGe_{3/7}Te_2$ is exemplary for the commensurate compounds in the series: after defining the strongest satellites to be the first-order satellites, and starting from the average structure that is common to all structures, one arrives quite easily at a model for the modulated structure.

The advantages of the superspace group approach as compared with a conventional supercell approach are primarily of a standardizing nature. All structures have the same basic unit cell and are fully characterized by their modulation wave vector and the global phase of the modulation wave. The structure refinement itself is not necessarily easier: the

number of independent parameters is the same as in a conventional refinement if the supercell symmetry is the same as the superspace group symmetry. A conventional refinement leads to the same results if the thermal parameters of like atoms are constrained to each other. It is expected that the larger the supercell the more difficult the conventional refinement would be, because of an increasing number of correlations.

$MA_xTe_2$ structures with $\frac{1}{3} \leqslant x \leqslant \frac{1}{2}$, whether commensurate or incommensurate, are simply described as ordered arrangements of the two extreme structures $MA_{1/3}Te_2$ and $MA_{1/2}Te_2$. It would be interesting to synthesize and determine the structures of e.g. $MA_{1/4}Te_2$ and $MA_{1/5}Te_2$ to answer two different sets of questions. Firstly: will they possess the same superspace group as the compounds with $\frac{1}{3} \leqslant x \leqslant \frac{1}{2}$ and will the building principle be different from those compounds? Secondly, how and at what stage will the environment of M change upon diminishing the A content of the system? The environment of M in the parent compound $MTe_2$ was reported to be octahedral [8], instead of trigonal prismatic as found in the phases described in this paper.

## Acknowledgments

The research of AvdL has been made possible by a grant from the Conseil Régional des Pays de la Loire. The authors thank Dr V Petříček (Institute of Physics, Praha) for stimulating discussions.

## References

[1] Monconduit L, Evain M, Boucher F, Brec R and Rouxel J 1992 Z. *Anorg. Allg. Chem.* **616** 1–6
[2] Canadell E, Monconduit L, Evain M, Brec R, Rouxel J and Whangbo M 1993 *Inorg. Chem.* **32** 10-2
[3] Evain M, Monconduit L, van der Lee A, Brec R and Rouxel J 1993 *New J. Chem.* at press
[4] Li J and Caroll P J 1992 *Mater. Res. Bull.* **27** 1073–81
[5] Li J, Badding E and DiSalvo F J 1992 *J. Alloys Comp.* **184** 257–63
[6] Van der Lee A, Evain M, Monconduit L, Brec R, Rouxel J and Petříček V 1993 *Acta Crystallogr.* B at press
[7] Monconduit L, Evain M, Brec R, Rouxel J and Canadell E 1993 *CR Acad. Sci., Paris* **314** 25–34
[8] Brown B E 1966 *Acta Crystallogr.* **20** 264–7
[9] Janssen T and Janner A 1987 *Adv. Phys.* **36** 519–624
[10] Van Smaalen S 1987 *Acta Crystallogr.* A **43** 202–7
[11] Van Smaalen S 1988 *Phys. Rev.* B **38** 9594–600
[12] Petříček V 1993 *JANA93-Programs for Modulated and Composite Crystals* (Praha, Czech Republic: Institute of Physics)
[13] *International Tables for X-ray Crystallography* 1974 vol I, IV, ed J A Ibers and W C Hamilton (Birmingham: Kynoch)
[14] *International Tables for X-ray Crystallography* 1992 vol C, ed A J C Wilson (Dordrecht: Kluwer)
[15] Yamamoto A and Nakazawa H 1982 *Acta Crystallogr.* A **38** 79–86
[16] Jobic S, Deniard P, Brec R, Rouxel J, Jouanneaux A and Fitch A N 1991 Z. *Anorg. Allg. Chem.* **589/599** 199–215
[17] Van der Lee A, Evain M, Mansuetto M, Monconduit L, Brec R and Rouxel J 1993 *J. Solid State Chem.* at press